

Application of Constant Amplitude Dynamic Tests for Life Prediction of Air Springs at Various Control Parameters

Tomaz Bešter* – Matija Fajdiga – Marko Nagode

University of Ljubljana, Faculty of Mechanical Engineering, Slovenia

Air spring manufactures use constant amplitude tests for the quality validation of air springs. The tests are very simple and the only information we get from them is that a spring is adequate if it passes the test and inadequate if it does not. One of the objectives of this article is to use these tests to make life predictions based on the standardised load spectrum. This prediction is made with force as the damage parameter. The second objective is to determine if it is possible to use experimental results obtained at one control parameter, e.g. force, to make life predictions for another control parameter, e.g. stress. With equations it is proved that such transformation is possible.

Keywords: vehicle suspension, air spring, load spectrum, dynamic tests, fatigue life

0 INTRODUCTION

Air spring assembly consists of a piston, bellows, a bed plate and a bumper (Fig. 1). Pressure inside the bellows and the piston shape determines air spring characteristics. An air spring can have progressive spring characteristic, which is most suitable for transport vehicles that are loaded with various loads during exploitation [1].

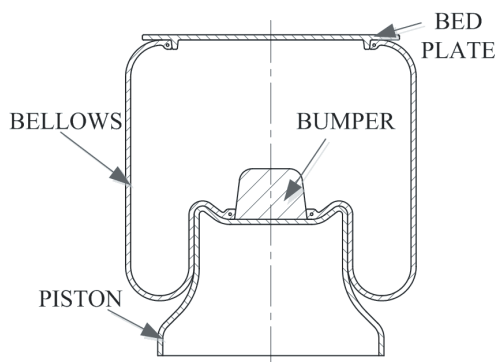


Fig. 1. Air spring

Air spring manufacturers have been testing springs with various static and dynamic experiments in order to verify spring quality. Dynamic tests usually have a constant amplitude and require a certain number of load cycles without critical damage on the air spring. If the spring successfully endures the test, critical damage on the spring does not occur and hence test results do not give exact information about fatigue life. In air spring fatigue tests, critical damage usually occurs on air spring bellows. In this article, the possibilities of obtaining SN-curves with modified constant amplitude tests will be examined. To make fatigue life predictions, loads on air springs and appropriate SN-curves must also be determined.

1 STANDARD LOAD SPECTRUM

For transport vehicles, standard load spectra were determined [2] and [3] which define dynamic wheel force $F_{z,dyn}$ on transport vehicles. Standard load spectrum has 1.5×10^8 load cycles, which corresponds to 500000 km driving distance with 300 load cycles per kilometre. Standardised load spectra have three driving modes: straight driving, cornering and braking. Based on wheel force measurements during exploitation, standard load spectrum was determined with the level crossing method. Dynamic force $F_{z,dyn}$ in standardized load spectra is expressed with dynamic load factor n_z which represents ratio between dynamic and static load $n_z = F_{z,dyn} / F_{z,sta}$. Dynamic load factor n_z depends on number of load cycles N and driving mode (Table 1, Fig. 2). For arbitrary static load $F_{z,sta}$ dynamic load $F_{z,dyn}$ can be determined with following equation:

$$F_{z,dyn} = n_z \cdot F_{z,sta} \quad (1)$$

Load ratio:

$$R_F = \frac{F_{min}}{F_{max}}, \quad (2)$$

where F_{min} is minimal force, and F_{max} is maximal force. During exploitation this ratio is changing. Load ratio range for all driving modes has been presented in Table 2.

When deformations are small and materials have linear characteristic, load ratio is equal to stress ratio:

$$R = R_F = R_\sigma = \frac{\sigma_{min}}{\sigma_{max}}, \quad (3)$$

where σ_{min} and σ_{max} are minimum and maximum stress. For high cycle fatigue, life calculation stress is

*Corr. Author's Address: University of Ljubljana, Faculty of Mechanical Engineering, Aškerčeva 6, SI-1000 Ljubljana, Slovenia, tomaz.bester@fs.uni-lj.si

usually used as the control parameter. When load ratio equals stress ratio, force can be used as the control parameter as well. On air springs, large deformations occur during exploitation and air spring bellows are made of polymer materials with nonlinear stress strain diagram [4] to [7]. Due to the geometric and material nonlinearities, Eq. (3) is not valid for air springs in general. This means fatigue life calculations with different control parameters will have different results. To compare fatigue life calculations with different parameters, SN-curves and Goodman diagrams would have to be determined for all control parameters in question. At least four experiments must be performed to design one Goodman diagram (Fig. 3). In this article, it will be shown how the Goodman diagram for one control parameter could be converted into the Goodman diagram for another control parameter that is not linearly dependent from the former parameter.

Table 1. Standard load spectra [2]

Driving mode	Load spectrum parameters $H_g = 1.5 \times 10^8$			
	Dynamic load factor n_z	H	H_e	SHAPE
Straight driving	2.0	$0.96 \cdot H_g$	$H \cdot 10^{-6}$	Linear distribution
Cornering Outer wheel Inner wheel	1.5 0.4	$0.04 \cdot H_g$	50	Normal distribution
Breaking	2.0	$5 \cdot 10^5$	10^4	Normal distribution

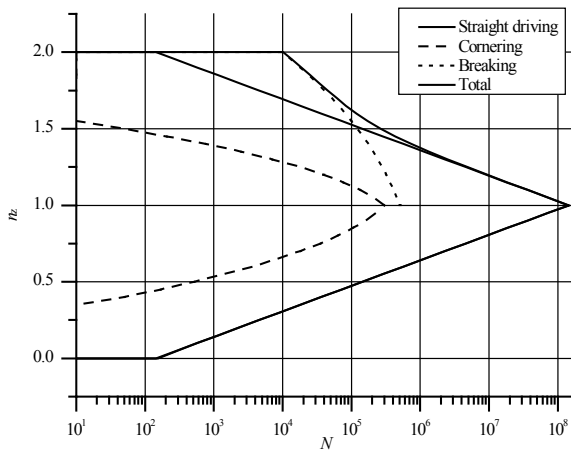


Fig. 2. Standard load spectra

Table 2. Load ratio ranges for various driving modes

Driving modes	R_f
Straight driving	0 to 1
Cornering	0.27 to 1
Breaking	0.5 to 1

2 DYNAMIC EXPERIMENTS AND FATIGUE LIFE

In the standardized load spectrum, load forces on wheels are defined. Wheel forces are transferred to air springs by suspension mechanism. As air spring forces are easily calculated, the easiest way to calculate fatigue life is to use force as a control parameter for the determination of SN-curves and the Goodman diagram. As load ratios of the standard load spectrum are in the range between 0 and 1, experiments for the determination of SN-curves and Goodman diagram must be in the same range.

For constant amplitude loads F_{a1R1} , F_{a2R1} , F_{a1R2} and F_{a2R2} the number of load cycles when critical damage occurs: N_{1R1} , N_{2R1} , N_{1R2} and N_{2R2} must be experimentally determined (Fig. 3). Those results allow to calculate SN-curves slope:

$$k_{R1} = \frac{\log N_{a1R1} - \log N_{a2R1}}{\log F_{a1R1} - \log F_{a2R1}} \quad (4)$$

$$k_{R2} = \frac{\log N_{a1R2} - \log N_{a2R2}}{\log F_{a1R2} - \log F_{a2R2}} \quad (5)$$

If fatigue limit is assumed to be at $N_D = 2 \times 10^6$, amplitude fatigue strength can be calculated for both dynamic factors:

$$F_{aDR1} = F_{a1R1} \left(\frac{N_D}{N_{1R1}} \right)^{\frac{1}{k_{R1}}} \quad (6)$$

$$F_{aDR2} = F_{a1R2} \left(\frac{N_D}{N_{1R2}} \right)^{\frac{1}{k_{R2}}} \quad (7)$$

From amplitude forces and load ratio, medium forces are calculated (for development of Eqs. (8) and (9) see the appendix):

$$F_{mDR1} = \frac{F_{aDR1}(1+R_1)}{(1-R_1)} \quad (8)$$

$$F_{mDR2} = \frac{F_{aDR2}(1+R_2)}{(1-R_2)} \quad (9)$$

and the gradient of the Goodman diagram:

$$M = \frac{F_{aDR2} - F_{aDR1}}{F_{mDR2} - F_{mDR1}} \quad (10)$$

When the gradient of the Goodman diagram is known, equivalent amplitude load F_{a1R1} with load ratio R_1 can be calculated (Fig. 4, for development of the Eq. (11) see the appendix):

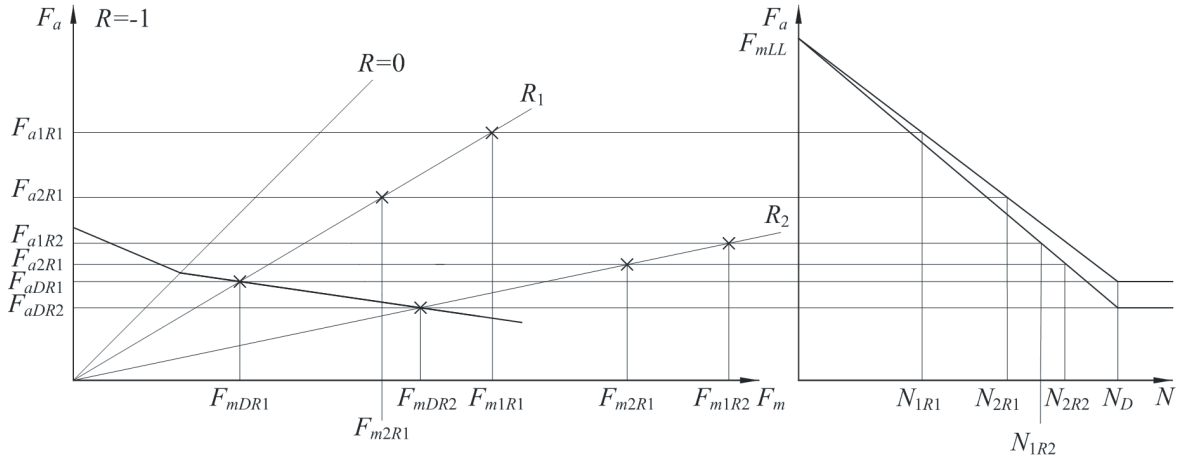


Fig. 3. Design of Goodman diagram

$$F_{a1R1} = F_{a1Ri} \frac{\left(1 + M \frac{(R_i + 1)}{(R_i - 1)}\right)}{\left(1 + M \frac{(R_1 + 1)}{(R_1 - 1)}\right)} \quad (11)$$

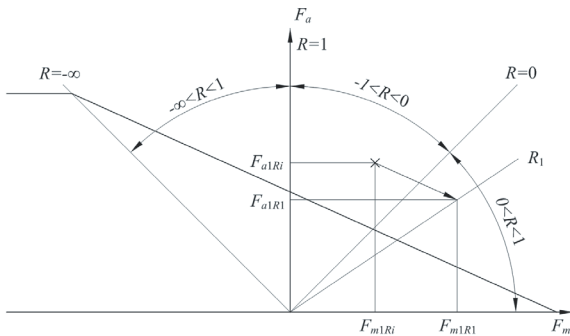


Fig. 4. Equivalent loads based on Goodman diagram [8]

Air spring manufacturers use various constant amplitude dynamic tests to validate quality and endurance of their air springs [9] and [10]. Two durability tests have been used in our research. In the first durability test, an air spring is loaded with the displacement amplitude ± 50 mm, at the frequency 3.3 Hz. The air spring must endure 2×10^6 load cycles without critical damage. In the second durability test, the displacement amplitude is ± 75 mm at the frequency 2 Hz, with the air spring having to endure 10^6 load cycles without critical damage. Both tests are stopped when the required number of load cycles is reached unless critical damage occurs first. If springs are tested until the critical damage occurs, two points on the SN-curve can be obtained. Air spring

characteristic was measured (Fig. 5) to determine the appropriate force amplitude for any displacement amplitude.

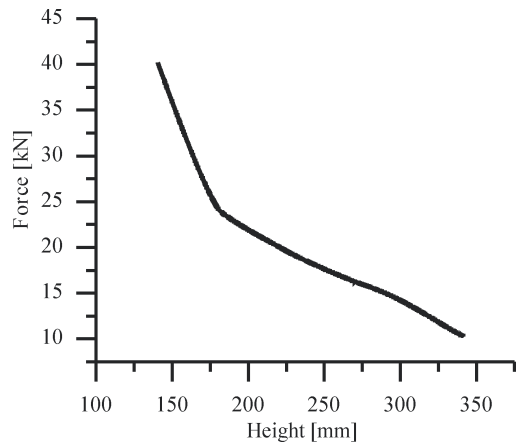


Fig. 5. Air spring characteristic

In the first durability test, the minimum required number of load cycles is the same as the fatigue limit. In the second durability test the minimum required number of load cycles is relatively near the fatigue limit. It is reasonable to use tests with higher amplitudes for determination of the remaining SN-curve points in order to reduce test time.

With two modified existing and two additional constant amplitude tests, two SN-curves and a Goodman diagram can be determined. This enables the transformation of any load to an equivalent load with the load ratio R_F of a known SN-curve.

An SN-curve can be approximately determined with the tensile strength force F_M and one dynamic test in the high cycle fatigue range because SN-curves with various load factors intersect near the tensile strength

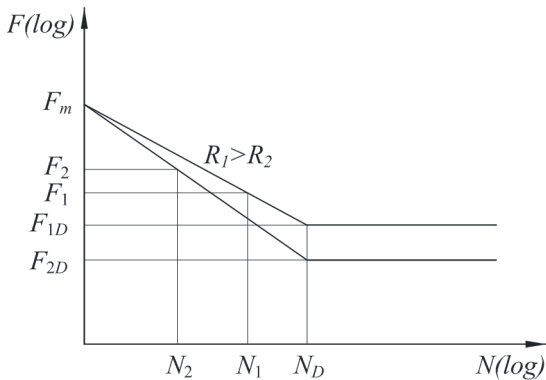


Fig. 6. Approximate SN-curves [11]

force (Fig. 6). An air spring’s maximum displacement is limited, therefore it is not possible to load a spring with a high enough load to cause the bellows to burst. The air spring bellows tensile strength cannot be directly determined, but it is possible to evaluate the tensile strength if pressure is increased in the spring’s bellows until it bursts and the maximum force is used as the tensile strength [11].

Once SN-curves are determined, fatigue life can be calculated with one of the damage accumulation rules [8] and [11]. The most frequently used linear accumulation rules are the original and elementary Palmgren-Miner rule and the Haibach rule (Fig. 7). In all linear accumulation rules, damage d_i is equal to the inverse number of load cycles when critical damage occurs. Total damage is:

$$d = \sum_{i=1}^n \frac{1}{N_{iR}} \quad (12)$$

In the described manner, damage was calculated for an air spring loaded with standardized load

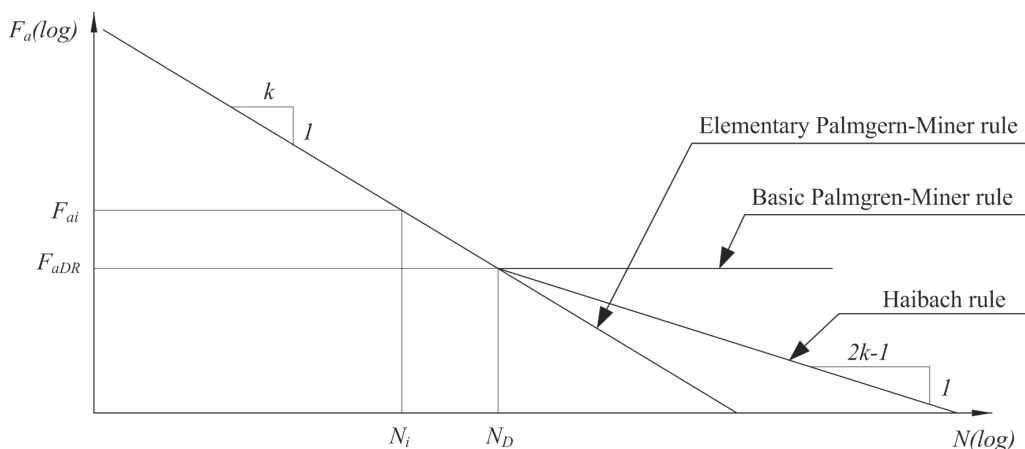


Fig. 7. SN-curves for original Palmgren-Miner, elementary Palmgren-Miner and Haibach rule [8]

spectrum (Table 3). The results show significant differences between accumulation rules.

When material has stress in the linear region of the stress strain diagram and deformations are small, the stress ratio is equal to the load ratio. Air springs are made of material with nonlinear stress strain diagram and are submitted to large deformations in most load cycles of the standard load spectrum. To evaluate the significance of those nonlinearities, life predictions with stress as the damage parameter should be made.

Table 3. Fatigue life

	Basic Palmgren-Miner rule	Elementary Palmgren-Miner rule	Haibach rule
Number of load cycles	9020073	3670064	5155576
Relative number of load cycles	1	0.40688	0.57157

3 LIFE PREDICTION WHEN DYNAMIC EXPERIMENTS HAVE DIFFERENT LOAD RATIOS

3.1 Determination of the Goodman Diagram from Four Dynamic Experiments with Different Load Ratios

A pair of experiments with equal load ratios when force is used as the control parameter (Fig. 3) will not have equal stress ratios (Fig. 8) due to the nonlinear relation between force and stress. It is not possible to determine SN-curves and the Goodman diagram directly with four experiments that have four different stress ratios. It will be shown that it is possible to solve the problem with a system of equations. The solution of this system can give all the data needed to determine the SN-curves and the Goodman diagram

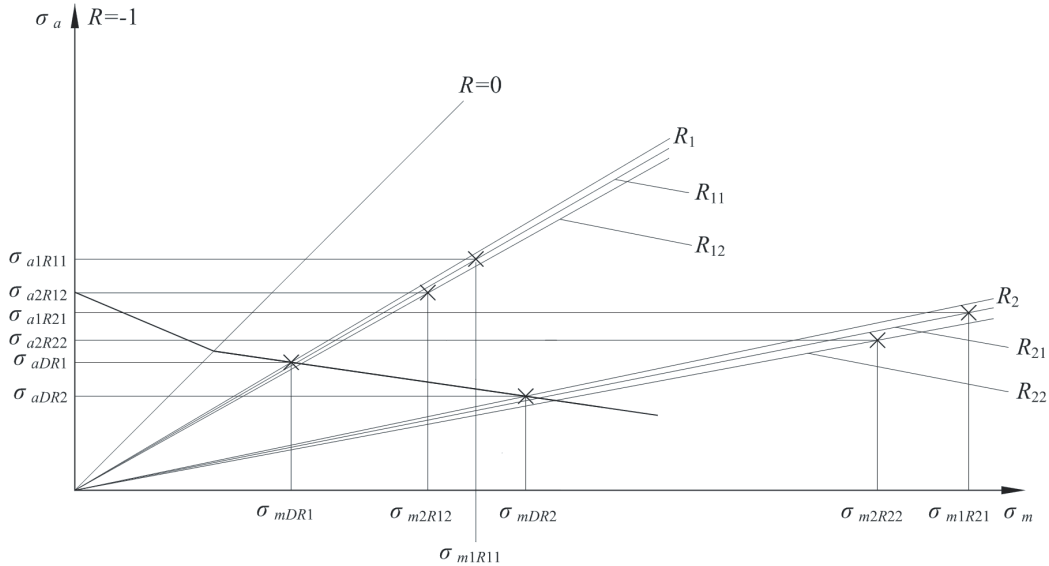


Fig. 8. Determination of the Goodman diagram from four dynamic tests

even if only four experiments with different stress ratios are available. Goodman diagram gradient M depends on two fatigue limit medium and amplitude stresses σ_{aDR11} , σ_{aDR21} , σ_{mDR11} and σ_{mDR21} (Table 4). To determine those stresses, two SN-curve gradients k_{R11} and k_{R21} are needed. To determine those gradients, it is necessary to obtain equivalent stresses with stress ratios R_{11} and R_{21} : σ_{m2R11} , σ_{m2R21} , σ_{a2R11} and σ_{a2R21} . To calculate equivalent stresses the gradient of the Goodman diagram M is needed. There are eleven unknowns. Eleven equations can be set, hence the unknowns can be determined by the equation system solution:

$$\sigma_{m2R11} = -\frac{(\sigma_{a2R12} - M\sigma_{m2R12}) \cdot (R_{11} + 1)}{((R_{11} - 1) + M(R_{11} + 1))}, \quad (13)$$

$$\sigma_{m2R21} = -\frac{(\sigma_{a2R22} - M\sigma_{m2R22}) \cdot (R_{21} + 1)}{((R_{21} - 1) + M(R_{21} + 1))}, \quad (14)$$

$$\sigma_{a2R11} = \frac{\sigma_{m2R11}(1 - R_{11})}{(R_{11} + 1)}, \quad (15)$$

$$\sigma_{a2R21} = \frac{\sigma_{m2R21}(1 - R_{21})}{(R_{21} + 1)}, \quad (16)$$

$$k_{R11} = \frac{\log N_{1R11} - \log N_{2R11}}{\log \sigma_{a1R11} - \log \sigma_{a2R11}}, \quad (17)$$

$$k_{R21} = \frac{\log N_{1R21} - \log N_{2R21}}{\log \sigma_{a1R21} - \log \sigma_{a2R21}}, \quad (18)$$

$$\sigma_{aD,R11} = \sigma_{a1R11} \left(\frac{N_D}{N_{1R11}} \right)^{\frac{1}{k_{R11}}}, \quad (19)$$

$$\sigma_{aDR21} = \sigma_{a1R21} \left(\frac{N_D}{N_{1R21}} \right)^{\frac{1}{k_{R21}}}, \quad (20)$$

$$\sigma_{mDR11} = \frac{\sigma_{aDR11}(1 + R_{11})}{(1 - R_{11})}, \quad (21)$$

$$\sigma_{mDR21} = \frac{\sigma_{aDR21}(1 + R_{21})}{(1 - R_{21})}, \quad (22)$$

$$M = \frac{\sigma_{aDR21} - \sigma_{aDR11}}{\sigma_{mDR21} - \sigma_{mDR11}}. \quad (23)$$

It is difficult to determine stresses on air spring bellows because large deformations and material nonlinearity must be considered. Despite these difficulties, precise enough stress-strain analyses were made [12] to [14]. As stresses in air spring bellows can be determined, known quantities in the system of equations are medium and amplitude stresses (Table 4). With part of equations being nonlinear, the system of equations does not have a simple analytical solution, but it can be solved numerically.

Table 4. Determination of the Goodman diagram from four dynamic tests– used quantities

Known quantities		Unknown quantities	
σ_{a1R11} [MPa]	Amplitude stress at F_{a1R1} [N] and F_{m1R1} [N]	σ_{aDR11} [MPa]	Amplitude fatigue strength at R_{11}
σ_{a2R12} [MPa]	Amplitude stress at F_{a2R1} [N] and F_{m2R1} [N]	σ_{aDR21} [MPa]	Amplitude fatigue strength at R_{21}
σ_{a1R21} [MPa]	Amplitude stress at F_{a2R1} [N] and F_{m2R1} [N]	σ_{mDR11} [MPa]	Medium stress at σ_{aDR11} [MPa]
σ_{a2R22} [MPa]	Amplitude stress at F_{a2R2} [N] and F_{m2R2} [N]	σ_{mDR21} [MPa]	Medium stress at σ_{aDR21} [MPa]
σ_{m1R11} [MPa]	Medium stress at F_{m1R1} [N] and F_{a1R1} [N]	k_{R11}	SN-curve gradient at R_{11}
σ_{m2R12} [MPa]	Medium stress at F_{m2R1} [N] and F_{a2R1} [N]	k_{R21}	SN-curve gradient at R_{21}
σ_{m1R21} [MPa]	Medium stress at F_{m1R2} [N] and F_{a1R2} [N]	σ_{a2R11} [MPa]	Equivalent amplitude stress for σ_{a2R12} [MPa] at R_{11}
σ_{m2R22} [MPa]	Medium stress at F_{m2R2} [N] and F_{a2R2} [N]	σ_{a2R21} [MPa]	Equivalent amplitude stress for σ_{a2R22} [MPa] at R_{21}
R_{11}	Stress ratio at F_{a1R1} [N] and F_{m1R1} [N]	σ_{m2R11} [MPa]	Equivalent medium stress for σ_{m2R12} [MPa] at R_{11}
R_{12}	Stress ratio at F_{a2R1} [N] and F_{m2R1} [N]	σ_{m2R21} [MPa]	Equivalent medium stress for σ_{m2R22} [MPa] at R_{21}
R_{21}	Stress ratio at F_{a2R1} [N] and F_{m2R1} [N]	M	Goodman diagram gradient
R_{22}	Stress ratio at F_{a2R2} [N] and F_{m2R2} [N]		
N_{1R11}	Number of load cycles when critical damage occurs at F_{a1R1} [N] and F_{m1R1} [N]		
N_{2R12}	Number of load cycles when critical damage occurs at F_{a1R1} [N] and F_{m1R1} [N]		
N_{1R21}	Number of load cycles when critical damage occurs at F_{a1R1} [N] and F_{m1R1} [N]		
N_{2R22}	Number of load cycles when critical damage occurs at F_{a1R1} [N] and F_{m1R1} [N]		
N_D	Fatigue limit		

3.2 Determination of the Goodman Diagram from Three Dynamic Experiments with Different Load Ratios

Although it is possible to determine the Goodman diagram from four dynamic tests with different dynamic factors, it is easier to use just three dynamic tests, but we have to omit the calculation in the first step to determine σ_{aD1} , k_{R1} and M . Equivalent stress σ_{a12} , σ_{m12} and σ_{a13} , σ_{m13} (Fig. 9, Table 5) can be calculated using following equations:

$$\frac{\sigma_{aD1}}{\sigma_{a1}} = \left(\frac{N_D}{N_1} \right)^{\frac{1}{k_1}}, \quad (24)$$

$$\frac{\sigma_{aD1}}{\sigma_{a12}} = \left(\frac{N_D}{N_2} \right)^{\frac{1}{k_1}}, \quad (25)$$

$$\frac{\sigma_{aD1}}{\sigma_{a13}} = \left(\frac{N_D}{N_3} \right)^{\frac{1}{k_1}}. \quad (26)$$

As σ_{a12} and σ_{a13} are not known in Eqs. (25) and (26), they must be expressed with known quantities. Based on the Goodman diagram equations can be written.

$$\sigma_{a12} - \sigma_{a2} = M(\sigma_{m12} - \sigma_{m2}), \quad (27)$$

$$\sigma_{a13} - \sigma_{a3} = M(\sigma_{m13} - \sigma_{m3}). \quad (28)$$

Medium stress can be written:

$$\sigma_{m12} = \frac{\sigma_{a12}(1 + R_1)}{(1 - R_1)}, \quad (29)$$

$$\sigma_{m13} = \frac{\sigma_{a13}(1 + R_1)}{(1 - R_1)}. \quad (30)$$

If Eqs. (29) and (30) are inserted in Eqs. (27) and (28), equations for σ_{a12} and σ_{a13} can be written using σ_{a2} , σ_{a3} , σ_{m2} , σ_{m3} , R_1 and M , where M is the only unknown:

$$\sigma_{a12} = \frac{(\sigma_{a2} - M\sigma_{m2})(1 - R_1)}{(1 - R_1) - M(1 + R_1)}, \quad (31)$$

$$\sigma_{a13} = \frac{(\sigma_{a3} - M\sigma_{m3})(1 - R_1)}{(1 - R_1) - M(1 + R_1)}. \quad (32)$$

If logarithms from Eqs. (24), to (26) are calculated and Eqs. (31) and (32) are used for σ_{a12} and σ_{a13} , a system of three equations and three unknowns is obtained:

$$\log \sigma_{aD1} - \log \sigma_{a1} = \frac{1}{k_1} (\log N_D - \log N_1), \quad (33)$$

$$\begin{aligned} \log \sigma_{aD1} - \log \left(\frac{(\sigma_{a2} - M\sigma_{m2})(1 - R_1)}{(1 - R_1) - M(1 + R_1)} \right) &= \\ = \frac{1}{k_1} (\log N_D - \log N_2), \end{aligned} \quad (34)$$

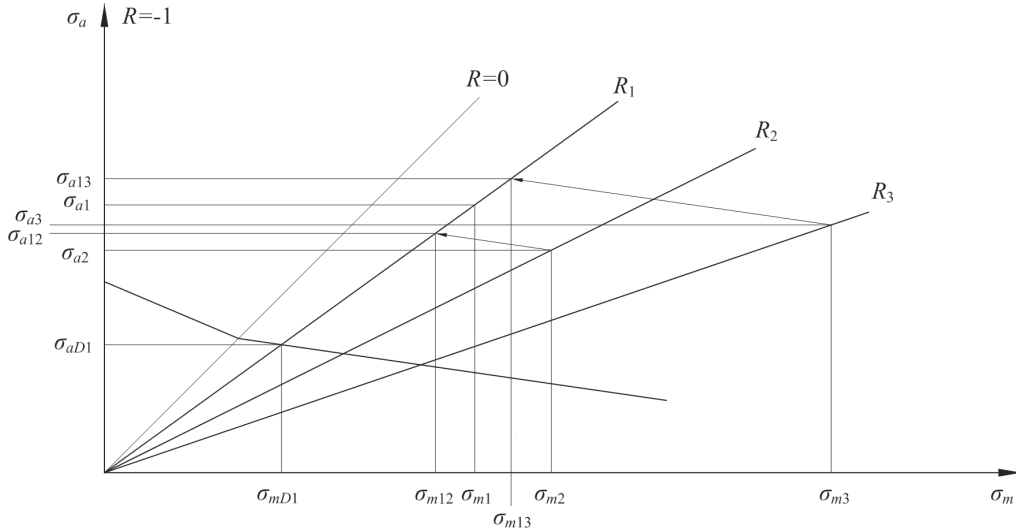


Fig. 9. Determination of the Goodman diagram from three dynamic tests

Table 5. Determination of the Goodman diagram from three dynamic tests – used quantities

Known quantities		Unknown quantities	
σ_{a1} [MPa]	Amplitude stress with stress ratio R_1	k_1	SN-curve gradient at R_1
σ_{a2} [MPa]	Amplitude stress with stress ratio R_2	M	Goodman diagram gradient
σ_{a3} [MPa]	Amplitude stress with stress ratio R_3	σ_{aD1} [MPa]	Amplitude fatigue strength at R_1
σ_{m1} [MPa]	Medium stress with stress ratio R_1	σ_{mD1} [MPa]	Amplitude fatigue strength at R_1
σ_{m2} [MPa]	Medium stress with stress ratio R_2	σ_{a12} [MPa]	Equivalent amplitude stress for σ_{a2} at R_1
σ_{m3} [MPa]	Medium stress with stress ratio R_3	σ_{a13} [MPa]	Equivalent amplitude stress for σ_{a3} at R_1
R_1	Stress ratio at σ_{a1} and σ_{m1}	σ_{m12} [MPa]	Equivalent medium stress for σ_{m2} at R_1
R_2	Stress ratio at σ_{a2} and σ_{m2}	σ_{m13} [MPa]	Equivalent medium stress for σ_{m3} at R_1
R_3	Stress ratio at σ_{a3} and σ_{m3}		
N_1	Number of load cycles when critical damage occurs at σ_{a1} and σ_{m1}		
N_2	Number of load cycles when critical damage occurs at σ_{a2} and σ_{m2}		
N_3	Number of load cycles when critical damage occurs at σ_{a3} and σ_{m3}		
N_D	Fatigue limit		

$$\log \sigma_{aD1} - \log \left(\frac{(\sigma_{a3} - M\sigma_{m3})(1 - R_1)}{(1 - R_1) - M(1 + R_1)} \right) = \frac{1}{k_1} (\log N_D - \log N_3). \quad (35)$$

$$\frac{1}{k_1} \left(\log \frac{N_1}{N_2} \right) + \log \left(\frac{(\sigma_{a2} - M\sigma_{m2})(1 - R_1)}{(1 - R_1) - M(1 + R_1)} \right) = \log \sigma_{a1}, \quad (37)$$

$$\frac{1}{k_1} \left(\log \frac{N_1}{N_3} \right) + \log \left(\frac{(\sigma_{a3} - M\sigma_{m3})(1 - R_1)}{(1 - R_1) - M(1 + R_1)} \right) = \log \sigma_{a1}. \quad (38)$$

From Eq. (33) $\log \sigma_{aD1}$ can be calculated:

$$\log \sigma_{aD1} = \log \sigma_{a1} + \frac{1}{k_1} (\log N_D - \log N_1), \quad (36)$$

and inserted into Eqs. (34) and (35). Thus two equations with two unknowns are obtained:

There is no simple analytical solution for Eqs. (37) and (38) but it is possible to calculate k_1 and M numerically. When k_1 is calculated, fatigue limit σ_{aD1} can be calculated with Eq. (36). With the Goodman diagram gradient M , any stress σ_{a1Ri} with arbitrary stress ratio R_i can be transformed to equivalent stress σ_{a1R1} with stress ratio R_1 and known SN-curve gradient k_1 :

6 APPENDIX

$$\sigma_{a1R1} = \sigma_{a1Ri} \frac{\left(1 + M \frac{(R_i + 1)}{(R_i - 1)}\right)}{\left(1 + M \frac{(R_1 + 1)}{(R_1 - 1)}\right)} \quad (39)$$

This enables to calculate equivalent stress for any load, e.g. σ_{a12} , σ_{a13} , etc. (Fig. 9).

4 CONCLUSION

Unchanged durability tests cannot be used to make fatigue life predictions, because unchanged tests are stopped when the required number of load cycles is reached. If those tests are performed until critical damage is reached and additional constant amplitude tests are made, two SN-curves, Goodman diagram and fatigue life prediction can be made. Fatigue life prediction was made with force as damage parameter using three damage accumulation rules. Various damage accumulation methods gave significantly different results. The elementary Palmgren-Miner rule and the Haibach modification take into account even loads that are smaller than the fatigue limit therefore those rules give shorter fatigue life predictions than the basic Palmgren-Miner rule. No tests were made with loads smaller than the fatigue limit therefore no estimation about the accuracy of damage accumulation rules in this range can be made.

Due to geometric and material nonlinearities, fatigue life calculations with force as the control parameter may be significantly different than fatigue life calculations with stress as the control parameter. The comparison of life predictions using different control parameters would be very time consuming and expensive as we would have to experimentally determine Goodman diagrams for all control parameters in question. With the equations we proved it is possible to transform the Goodman diagram for one control parameter, e.g. force, into the Goodman diagram for another control parameter, e.g. stress. The transformation of the Goodman diagram to arbitrary control parameters makes further research of the influence of control parameters on fatigue life much quicker and less expensive.

5 ACKNOWLEDGMENT

The authors appreciate the support provided by the Veyance Technologies Europe, d.o.o.

Development of the medium force equation (Eqs. (8) and (9)). Analogue equations are used for medium stress (Eqs. (29) and (30)).

$F_{D \max}$ – maximum force

$F_{D \min}$ – minimum force

F_{mDRi} – medium force with load ratio R_i

F_{aDRi} – amplitude force with load ratio R_i

$$R_i = \frac{F_{D \min}}{F_{D \max}} = \frac{F_{mDRi} - F_{aDRi}}{F_{mDRi} + F_{aDRi}},$$

$$R_i \cdot F_{mDRi} + R_i \cdot F_{aDRi} = F_{mDRi} - F_{aDRi},$$

$$R_i \cdot F_{mDRi} - F_{mDRi} = -R_i \cdot F_{aDRi} - F_{aDRi},$$

$$F_{mDRi} (R_i - 1) = -F_{aDRi} (R_i + 1),$$

$$F_{mDRi} = -F_{aDRi} \frac{(R_i + 1)}{(R_i - 1)} = F_{aDRi} \frac{(1 + R_i)}{(1 - R_i)}.$$

Development of the equivalent amplitude force equation (Eq (11), Fig. 4). Analogue equation is used for equivalent amplitude stress (Eq. (39)).

F_{a1Ri} – amplitude load with load ratio R_i

F_{a1R1} – equivalent amplitude load with load ratio R_1

F_{m1Ri} – medium load with load ratio R_i

F_{m1R1} – equivalent medium load with load ratio R_1

$$M = \frac{F_{a1R1} - F_{a1Ri}}{F_{m1R1} - F_{m1Ri}},$$

$$F_{a1R1} - F_{a1Ri} = M (F_{m1R1} - F_{m1Ri}),$$

$$F_{a1R1} - F_{a1Ri} = M \left(-F_{a1R1} \frac{(R_1 + 1)}{(R_1 - 1)} - F_{m1Ri} \right),$$

$$F_{a1R1} + M \cdot F_{a1R1} \frac{(R_1 + 1)}{(R_1 - 1)} = F_{a1Ri} - M \cdot F_{m1Ri},$$

$$F_{a1R1} \left(1 + M \frac{(R_1 + 1)}{(R_1 - 1)} \right) = F_{a1Ri} + M \cdot F_{m1Ri} \frac{(R_1 + 1)}{(R_1 - 1)},$$

$$F_{a1R1} = F_{a1Ri} \frac{\left(1 + M \frac{(R_1 + 1)}{(R_1 - 1)}\right)}{\left(1 + M \frac{(R_i + 1)}{(R_i - 1)}\right)}.$$

7 REFERENCES

- [1] Pirnat, M., Savšek, Z., Boltežar, M. (2011). Measuring dynamic loads on a foldable city bicycle. *Strojniški vestnik - Journal of Mechanical Engineering*, vol. 57, no. 1, p. 21-26, DOI:10.5545/sv-jme.2009.149.21-26, 2011.
- [2] Neugebauer, J.R., Grubisic, V., Fischer, G. (1989). *Procedure For Design Optimization And Durability Life Approval Of Truck Axles And Axle Assemblies*. SAE Technical Paper, 892535.
- [3] Heuler, P., Klätschke, H. (2005). Generation and use of standardised load spectra and load-time histories. *International Journal of Fatigue*, vol. 27, no. 8, p. 974-990, DOI:10.1016/j.ijfatigue.2004.09.012.
- [4] Oman, S., Nagode, M., Fajdiga, M. (2009). The material characterization of the air spring bellow sealing layer. *Materials & Design*, vol. 30, no. 4, p. 1141-1150, DOI:10.1016/j.matdes.2008.06.035.
- [5] Shaw, M.T., MacKnight, W.J. (2005). *Introduction to Polymer Viscoelasticity, 3rd ed.* John Wiley & Sons, Hoboken, DOI:10.1002/0471741833.
- [6] Tschoegl, N.W., Knauss, W.G., Emri, I. (2002). The effect of temperature and pressure on the mechanical properties of thermo- and/or piezorheologically simple polymeric materials in thermodynamic equilibrium – A critical review. *Mechanics of Time-Dependent Materials*, vol. 6, no. 1, p. 53-99, DOI:10.1023/A:1014421519100.
- [7] Gent, A. (2012). *Engineering With Rubber*. Carl Hanser Verlag, Munich, DOI:10.3139/9783446428713.
- [8] *LMS Falanx Theory Manual version 2.9*. (2000). LMS Durability Technologies, Leuven.
- [9] *Air Spring - Installation Requirement* (2008). Mack Trucks, Allentown.
- [10] *Durability-Flex Life* (2009). Goodyear Tire and Rubber Company, Green.
- [11] Ellyin, F. (1997). *Fatigue Damage, Crack Growth And Life Prediction*. Chapman&Hall, London.
- [12] Oman, S., Fajdiga, M., Nagode, M. (2010). Estimation of air-spring life based on accelerated experiments. *Materials and Design*, vol. 31, no. 8, p. 3859-3868, DOI:10.1016/j.matdes.2010.03.044.
- [13] Hackenschmidt, R., Alber-Laukant, B., Rieg, F. (2011). Simulating nonlinear materials under centrifugal forces. *Strojniški vestnik - Journal of Mechanical Engineering*, vol. 57, no. 7-8, p. 531-538, DOI:10.5545/sv-jme.2011.013.
- [14] Oman, S., Nagode, M. (2013). On the influence of the cord angle on air-spring fatigue life. *Engineering Failure Analysis*, vol. 27, p. 61-73, DOI:10.1016/j.engfailanal.2012.09.002.